ORE CHARACTERISTICS THAT AFFECT BREAKAGE DURING GRINDING

W. PETRUK and M.M. SMITH
Mineral Processing Laboratory

MINERAL SCIENCES LABORATORIES
CANMET REPORT CM88-5E

May 1988

Available in Canada through

Associated Bookstores
and other booksellers

or by mail from

Canadian Government Publishing Centre
Supply and Services Canada
Ottawa, Canada K1A 0S9

Catalogue No. M38-13/88-5E
ISBN 0-660-13121-8

ORE CHARACTERISTICS THAT AFFECT BREAKAGE DURING GRINDING

by

W. Petruk* and M.M. Smith**

Abstract

A base metal ore from the New Brunswick No. 12 deposit in the Bathurst area, New Brunswick, was studied to determine the mechanics of ore breakage during grinding. The ore was ground for different periods of time in a laboratory ball mill, and both the unbroken ore and ground products were analyzed by a variety of image analysis techniques, including modifications of fractal analyses.

The results show that the mode of breakage is strongly influenced by the behaviour of pyrite. Initial grinding breaks pyrite along grain boundaries (i.e., preferential breakage), and the process continues until most of the poorly to moderately bonded pyrite grains have been separated. Further grinding breaks pyrite across grain boundaries (random breakage) and chips edges off particles. This observation indicates that liberation of interstitial minerals among pyrite in base metal ores is more dependent upon preferential breakage, along pyrite grain boundaries, than upon random breakage of the ore, as generally assumed. Consequently, the interstitial minerals among pyrite, which are generally smaller than the pyrite grains, will be liberated at a coarser grind than would be expected if the ore broke randomly.

KEYWORDS: liberation, texture analysis, image analysis, grain erosion, grain dilation.

---

*Senior Research Scientist and **Post-doctoral fellow, Process Mineralogy Section, Mineral Sciences Laboratories, CANMET, Energy, Mines and Resources Canada, Ottawa, Ontario K1A 0G1.

CARACTÉRISTIQUES DU MINERAI AFFECTANT LA RUPTURE PENDANT LE BROYAGE

par

W. Petruk* et M.M. Smith**

Résumé

On a analysé un minerai de métaux de base provenant du dépôt n° 12 de la région de Bathurst au Nouveau-Brunswick afin de déterminer la mécanique de la rupture pendant le broyage. Le minerai a été broyé pendant des périodes plus ou moins longues dans un broyeur à boulets. Le minerai non fragmenté et les produits broyés ont fait l'objet d'une étude qui a été réalisée par diverses techniques d'analyse d'images, y compris des analyses fractales modifiées.

Les résultats indiquent que le mode de rupture est très influencé par le comportement de la pyrite. Le broyage préliminaire fragmente la pyrite le long des joints intergranulaires (i.e., rupture préférentielle) et le procédé continu jusqu'à ce que la majorité des grains de pyrite, peu ou moyennement agglomérés, soient séparés. Un broyage plus poussé brise la pyrite le long des joints intergranulaires (rupture aléatoire) et fragmente les particules. Ce fait indique que la libération des minéraux interstitiels retrouvés parmi la pyrite dans le minerai de métaux de base repose davantage sur la rupture préférentielle, le long des joints intergranulaires des grains de pyrite, que sur la rupture aléatoire du minerai, comme on le pense en général. Par conséquent, les minéraux interstitiels retrouvés parmi la pyrite sont habituellement plus petits que les grains de pyrite et seront libérés sous une forme plus grossière que prévue dans le cas d'une fragmentation aléatoire du minerai.

MOTS CLÉ : libération; analyse de la texture; analyse d'image; érosion du grain; dilatation du grain.

---

*Chercheur scientifique principal et **boursier-post doctoral, Section de la minéralogie appliquée, Laboratoires des sciences minérales, CANMET, Énergie, Mines et Ressources Canada, Ottawa (Ontario) K1A 0G1.

CONTENTS

TABLES

FIGURES

INTRODUCTION

The mechanics of ore breakage during grinding is not understood well enough to develop a liberation model that gives liberations. Existing liberation models assume random breakage for predicting mineral liberations (1, 2, 3) and show good correlations when random breakage is obvious. On the other hand, the correlations are poor when random breakage is not apparent (4, 5, 6, 7). This suggests that both random and preferential breakage occur during crushing and grinding. Breakage is assumed to occur (a) along incipient fractures (preferential breakage), (b) along layers and veinlets of soft minerals (preferential breakage), (c) along grain boundaries (preferential breakage), (d) across grain boundaries (random breakage), and (e) by chipping edges off particles (random breakage). The extent to which each type of breakage occurs during grinding of a base metal ore in a ball mill was studied by analyzing the ore from the Brunswick No. 12 deposit of Brunswick Mining and Smelting Corp. Ltd. (BMS) near Bathurst, N.B. Grinding tests were conducted, and polished sections of the screened fractions from the grinding tests as well as of unbroken ore pieces were analyzed with the image analysis system.

MINERAL IDENTITIES AND SIZE DISTRIBUTIONS IN UNBROKEN ORE

A sample of rod mill feed (RMF), consisting of −2.5 cm pieces, was obtained from BMS in August 1986. Twenty 2.5 cm pieces were randomly selected, and polished sections were prepared. Eleven polished sections were analyzed with the image analysis system to determine mineral identities, quantities and size distributions (Table 1). The pyrite size distribution could not be analyzed directly because most of the pyrite occurs as aggregates of grains; consequently, a grain boundary reconstruction technique (8) was used (Fig. 1). The reconstructed image displays each pyrite grain as a discrete individual and thereby permits measurement of its size. The size distribution was determined by chord size analyses of the reconstructed pyrite grains in images of the ore (8) (Table 2, col 8).

GRINDING TESTS

The RMF sample was ground in a laboratory rod mill to −1.7 mm (−10 mesh) and was split into five 2−kg samples. In a ball mill using steel balls, one sample was ground for 15 minutes, the second for 30 minutes, the third for 45 minutes, the fourth for 60 minutes and the fifth for 90 minutes. Each ground product was sieved with a series of screens from 600 to 37.5 μm (28 to 400 mesh). Grain sizes within the −37.5 μm fractions were determined with the image analyzer. Size analyses of the BMS grinding−circuit discharge for September 1976 (9) and December 1986 (Table 2) were also obtained.

A comparison of columns 3, 8, 9 and 10 in Table 2 shows that similar size distributions were obtained for material from the 15 minute grind in the laboratory ball mill, for the BMS grinding−circuit discharges, and for pyrite grains in the unbroken ore (Fig. 2). This similarity indicates that ball−mill grinding of BMS ore breaks it into particles that are approximately the same size as the pyrite grains

Table 1 – Mineral identities and mineral quantities

Mineral	Unbroken ore	15 min	30 min	45 min	60 min	90 min
Silicates*	18.0	22.9	20.9	23.3	21.0	24.0
Pyrite**	60.3	52.1	56.1	54.5	58.1	55.3
Pyrrhotite	0.9	0.5	0.4	0.2	0.3	0.4
Chalcopyrite	0.8	0.7	0.5	0.6	0.3	0.4
Sphalerite	14.5	16.4	16.3	15.8	15.1	14.5
Arsenopyrite***	1.9	2.7	2.3	2.1	2.1	2.3
Galena	3.6	4.7	3.5	3.5	3.1	3.1

*Mainly quartz, but includes mica, feldspar, amphibole, chlorite, calcite, siderite, dolomite, apatite and goethite.

**About 99.9% pyrite, but may include magnetite, hematite and zircon.

***Includes barite, tetrahedrite, cassiterite, boulangerite and pyrargyrite.

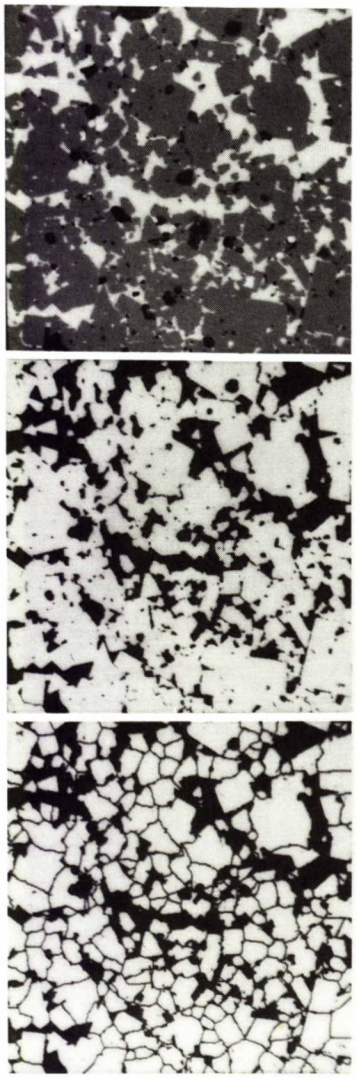

Fig. 1 – (a) A backscattered electron (BSE) micrograph of a base metal ore showing pyrite (grey), sphalerite (dull white), gangue (black) and galena (bright white spots). (b) A binary image generated by the image analysis system for the pyrite in Figure 1a. (c) Binary image of Figure 1b with reconstructed grain boundaries.

Table 2 – Size distributions* of samples

1 Size (μm)	2 Head	3 15 min	4 30 min	5 45 min	6 60 min	7 90 min	8 Pyrite underground	9 BMS 9/76	10 BMS 12/86
3.4	0.72	3.65	2.87	2.74	4.12	5.29	2.0	2.9	
4.7	1.54	4.86	6.24	6.08	9.66	11.93	3.9	5.9	
6.7	2.84	14.01	11.57	11.42	17.81	21.82	7.6	8.9	
9.3	4.84	21.47	19.43	20.12	30.00	36.70	13.4	13.3	
13.3	7.56	29.77	30.94	33.87	46.95	53.44	20.2	21.0	25.88
18.7	10.43	39.20	46.19	51.55	67.03	70.87	30.8	31.7	31.77
26.6	12.41	49.26	63.31	70.75	85.12	87.55	43.0	43.1	41.84
37.5	14.1	56.48	77.80	89.30	95.20	97.90	55.8	59.9	53.83
53	17.6	71.92	92.25	97.76	99.42	99.60	68.6	77.2	62.73
75	19.7	82.74	96.99	99.27	99.87	99.80	80.1	85.6	81.61
106	22.3	92.34	99.29	99.87	99.97	99.93	88.9	90.2	87.81
150	25.2	97.57	99.84	99.95	100.00	99.98	94.3		94.32
212	29.0	99.40	99.89	100.00		100.00	97.0	97.1	97.08
300	33.6	99.60	99.92						
424	48.9	99.65	99.95						
+424	51.5	00.35	00.05	0.00	0.00	0.00	0.0	0.0	0.00

* = % smaller than

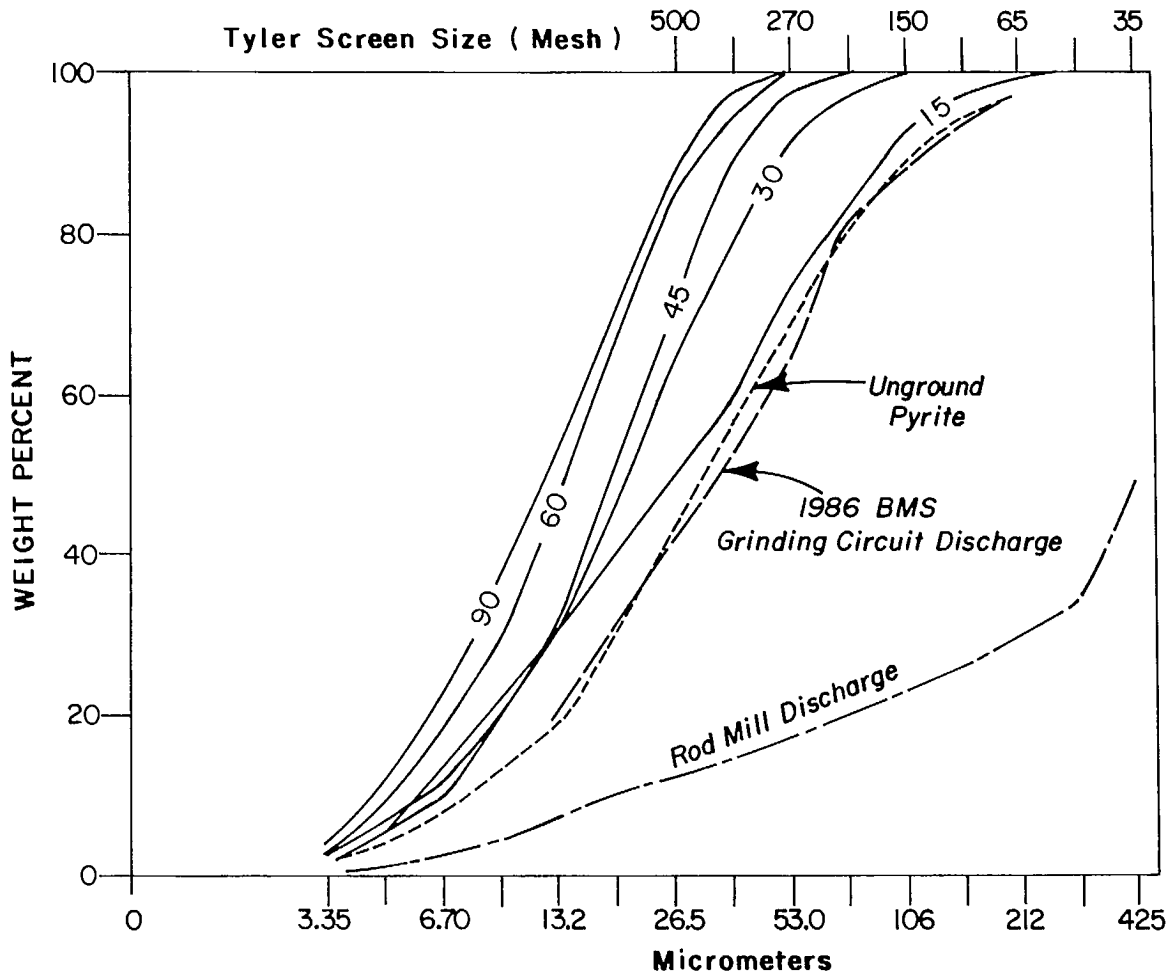

Fig. 2 – Particle size analysis of the rod mill discharge, ore ground for various time intervals (15, 30, 45, 60 and 90 minutes), flotation feed to BMS concentrator, and pyrite in underground ore.

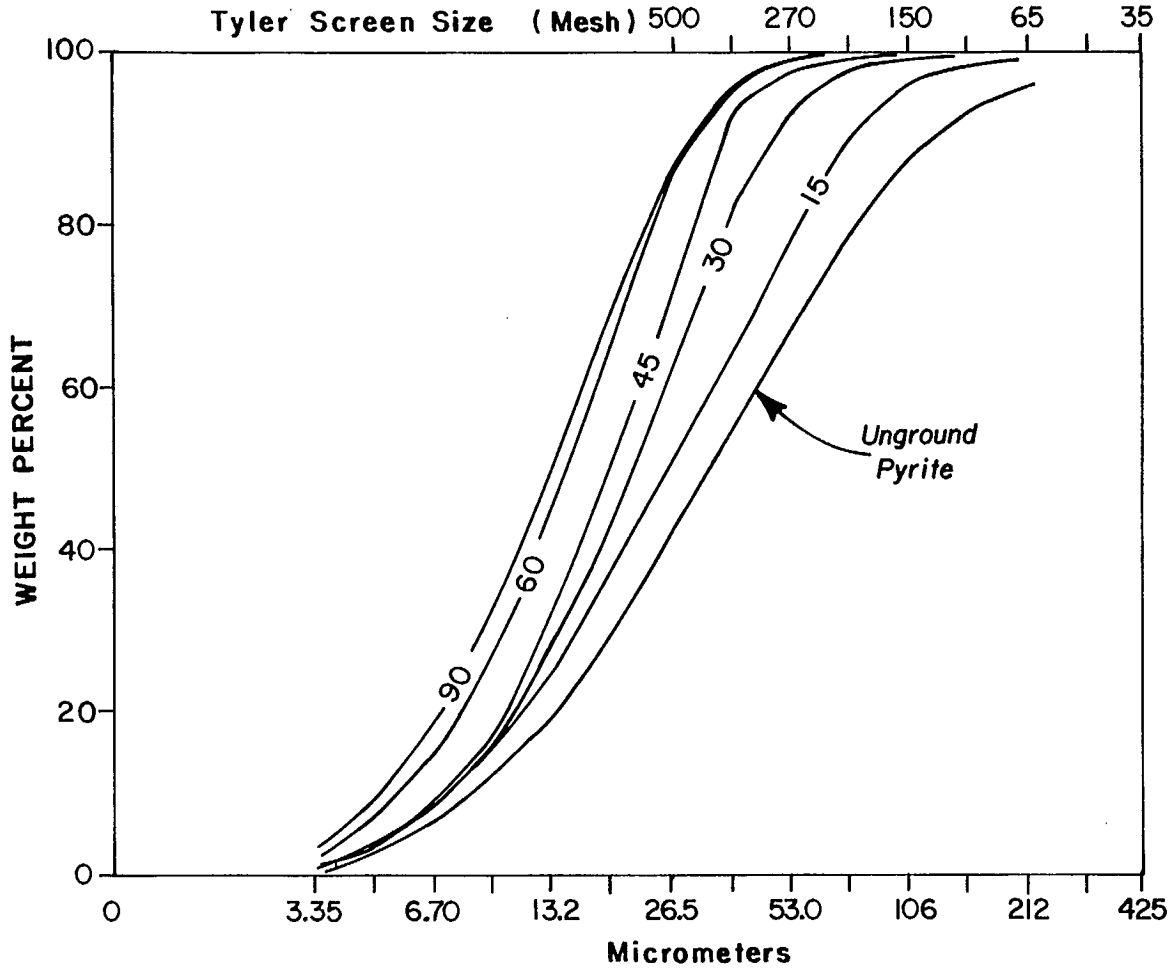

Fig. 3 – Particle size analysis of pyrite in ore ground for 15, 30, 45, 60 and 90 minutes, and of pyrite in underground ore.

in the ore. To determine whether this observation applies to base metal ores in general or is unique to the BMS ore, tests were conducted on base metal ores from the Trout Lake deposit of Hudson Bay Mining and Smelting in Manitoba and from the Curragh Resources deposit (Faro deposit) in Yukon. A similar relationship was observed between the size distributions for the ground products and those for pyrite in the unbroken ore for the Trout Lake deposit but not for the Curragh Resources deposit. The Trout Lake ore is pyrite– and quartz–rich, and, as in BMS ore, the sphalerite is coarser grained than pyrite. In contrast, the Curragh Resources ore has a high amount of mafic minerals, and the sphalerite is finer grained than pyrite. These observations suggest that when pyrite–rich base metal ores are ground in either a laboratory mill for 15 minutes, or in a grinding circuit of a commercial mill, the size distributions for the particles in the ground ore are approximately the same as those for the pyrite grains in the unbroken ore. Further grinding in a laboratory mill will break the particles into smaller sizes.

An assessment of the size distribution curves from the different grinds (Fig. 2) shows the following:

1. Most of the particles in the 15 minute grind sample are smaller than 150 μm in diameter, which is equivalent to the maximum size of the pyrite grains in the ore.

2. The 0 to 13.3 μm particles in samples of the 15, 30 and 45 minute grinds have approximately the same size distributions, which suggests that grains ranging in diameter from 0 to 13.3 μm have a distinct property.

3. The top ends of the cumulative size distribution curves for the 30 and 45 minute grinds have moved from the 106 to 150 μm size range observed for the 15 minute grind towards the 37.5 to 53 μm size range. This observation suggests that the ore has textures which cause it to break into particles of 37.5 to 53 μm in diameter.

4. The cumulative size distribution curves for the 45, 60 and 90 minute grinds are parallel and are closely spaced for the 60 and 90 minute grinds. This suggests that most of the pyrite grains have been broken apart at the 45 minute grind (i.e., preferential breakage was completed) and that breakage at the 60 and 90 minute grinds occurred largely by breaking pyrite grains across grain boundaries (random breakage).

5. The size distribution curves for the free pyrite grains (determined by image analysis) in the products from the 15, 30, 45, 60 and 90 minute grinds are similar to the size distribution curves for the ground ore. This similarity substantiates the interpretation that the pyrite grain sizes and textures influence breakage of base metal ores.

MINERAL QUANTITIES IN GROUND PRODUCTS

Mineral quantities were determined with the image analyzer for each screened fraction from each grinding test. The results show distinct changes in mineral quantities at the 104 to 147 and 36.8 to

52.1 μm size range (Fig. 4). In the rod mill discharge, where the minerals occur largely in multi-mineral grains, the quantity of each mineral is approximately the same in each screened fraction. In the 15 and 30 minute grind material, the quantity of pyrite is decreased and that of silicates is increased in the 104 to 147 μm and coarser fractions. This observation indicates that since most of the pyrite in the unbroken ore is finer grained than 150 μm in diameter (from size analysis of pyrite in unbroken ore), the pyrite breaks into particles that are smaller than 150 μm in diameter. Consequently, the amount of pyrite in coarser sized fractions is reduced. The 60 and 90 minute grinds show a depletion of pyrite in fractions that are coarser grained than 44 μm, which indicates that nearly all pyrite grains larger than 44 μm have been broken, and their quantities have been reduced. This observation suggests that the ore has a property that causes it to break into particles that are smaller than 44 μm in diameter.

TEXTURE ANALYSES

To determine whether the 0 to 13 and the 37.5 to 53 μm size ranges are influenced by ore properties, four techniques of measuring the interrelations between different sized pyrite grains by image analysis were developed and tested. The techniques are:

1. sequential grain erosion with field perimeter measurement;
2. sequential grain dilation with field perimeter measurement;
3. combination of grain erosion and grain dilation with field perimeter measurements; and
4. area perimeter measurement of each particle.

To obtain statistically valid data, 20 fields (5000 to 10 000 grains) were measured for each polished section. The data from the 11 polished sections were combined (55 000 to 110 000 grains were measured). In tests of specific grain interrelations observed in only one field of view, 250 to 500 grains were measured (10).

Sequential Grain Erosion with Field Perimeter Measurements

An erosion technique was developed as a modification of a fractal analysis technique (10, 11). It involves successively stripping a layer (erosion), one pixel wide, from the image of each grain in the field of view, and measuring the total perimeter for the grains in the image after each erosion. The procedure was continued for 16 erosion steps (Fig. 5). The field perimeter measured for each erosion step was plotted as ln perimeter versus ln steplength (Fig. 6). The steplength depends upon the magnification; under the analytical conditions used (magnification = 150x) the grain diameter decreased 3 μm for each steplength. The slope of the resulting curve for each step was determined, and breaks in slope were noted. The largest break occurred at 42 μm, which indicates a change in interrelations between the large and the small pyrite grains. Since the 42 μm size falls within the 37.5 to 53 μm size range noted from the grinding and mineral quantity data, it is interpreted that the change in interrelations of pyrite grains affects breakage during grinding.

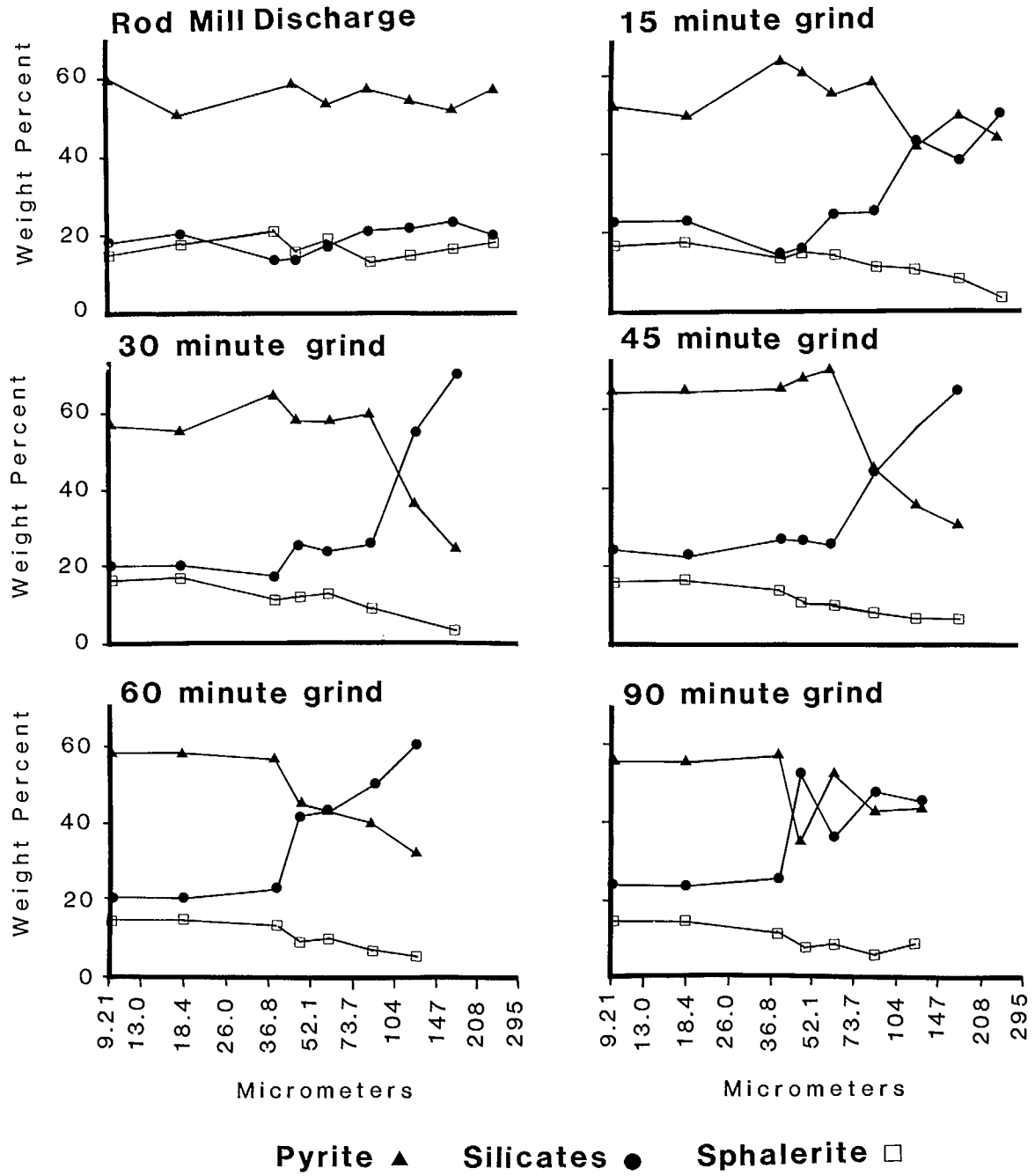

Fig. 4 – Mineral quantities in screened fractions of the rod mill discharge, the 15, 30, 45, 60 and 90 minute grinds.

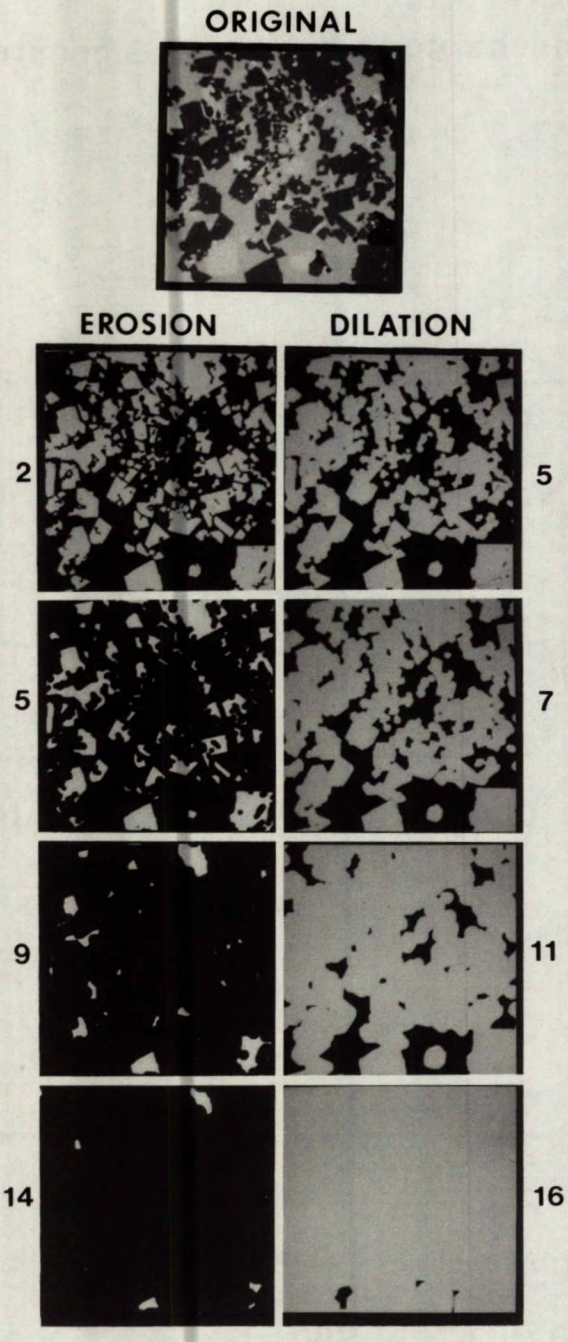

Fig. 5 – A BSE image of a base metal ore transferred to the image analysis system. Pyrite is grey; sphalerite is light grey; and gangue is black. The left column represents views after the image had been eroded two, five, nine and fourteen times. The right column represents views after the image had been dilated five, seven, eleven and sixteen times.

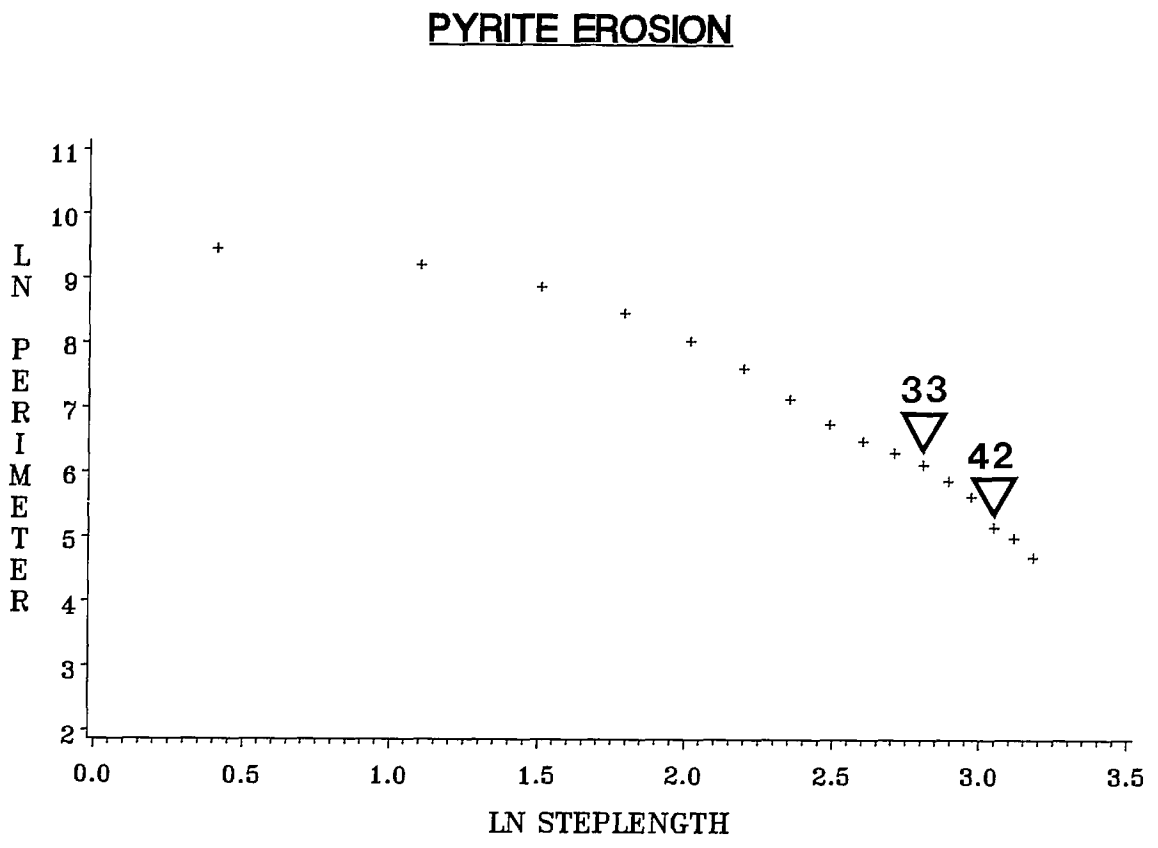

Fig. 6 – A plot of the ln perimeter versus ln steplength. Each step represents an erosion of 1.5 μm around each grain or 3 μm in grain diameter. The largest breaks in slope occur at 33 and 42 μm.

Erosion removes irregularities from the outlines of grain images and reduces the size of the grain images. Furthermore, the grain disappears when the grain diameter is smaller than the size of the combined erosion steps (Fig. 5). The reduction in slope of the ln perimeter versus ln steplength is therefore a measure of both grain surface irregularities and the grain size (9).

Grain Dilation with Field Perimeter Measurements

A grain dilation technique that used a procedure similar to the grain erosion techniques was also developed. The image for each grain was successively dilated one pixel (Fig. 5), and the field perimeter for the grains was measured after each dilation. The data were plotted as ln perimeter versus ln dilation step, and the slopes of the resulting curves between dilation steps were calculated. For the image depicted in Figure 5 (one field of view) the largest breaks in slope with dilation occurred at 9 and 33 μm (Fig. 7).

Dilation modifies the grain image by increasing the grain diameter and rounding the grain outline. When grains are widely spaced, each dilation step increases the field perimeter by a constant factor and the data produce a straight line when plotted as ln perimeter versus ln steplength. On the other hand, when grains are closely spaced, dilation combines the grains by filling the intergranular spaces and thereby reduces the field perimeter. The combined data for all fields analyzed in the 11 polished sections show that the largest break in slope is at 6 μm which suggests that most of the interstitial spaces between pyrite grains are narrower than 6 μm.

Erosion Dilation with Field Perimeter Measurements

To further test whether changes in pyrite textures are present, the average slope between each dilation step for the 11 samples was plotted versus the average slope between each erosion step. The combination of erosion and dilation techniques provides a measure of grain size, roughness and separation. The erosion dilation technique may therefore be a valid method of determining grain interrelations. It was observed that the points were separated whenever there was a large change in slope. The combined data for pyrite (Fig. 8) show a large separation at 6 μm and marked separations at 12 and 42 μm. The separations occur at sizes that fall within the size ranges of 0 to 13 and 37.5 to 53 μm observed in the grinding tests, and indicate that breakage of pyrite is related to grain sizes, roughness and separations.

Area–Perimeter Measurements

The area (A) and perimeter (P) of 1472 particles in one sample were measured and the data were plotted as P^2/A versus A (Fig. 9). The test was conducted to determine whether particle shape and size affect ore breakage. A square has a P^2/A value of 16, whereas a circle has a P^2/A value of 12.57. The value increases with both increasing grain roughness and increasing aspect ratio. A visual correlation of P^2/A to grain shapes in the images indicates that values of 16 to 45 correspond to grains that, in polished sections, appear approximately as squares. The scatter diagram of P^2/A versus A (Fig. 9b) shows that some grains smaller than about 100 μm^2 (diameter = 10 μm) are circular;

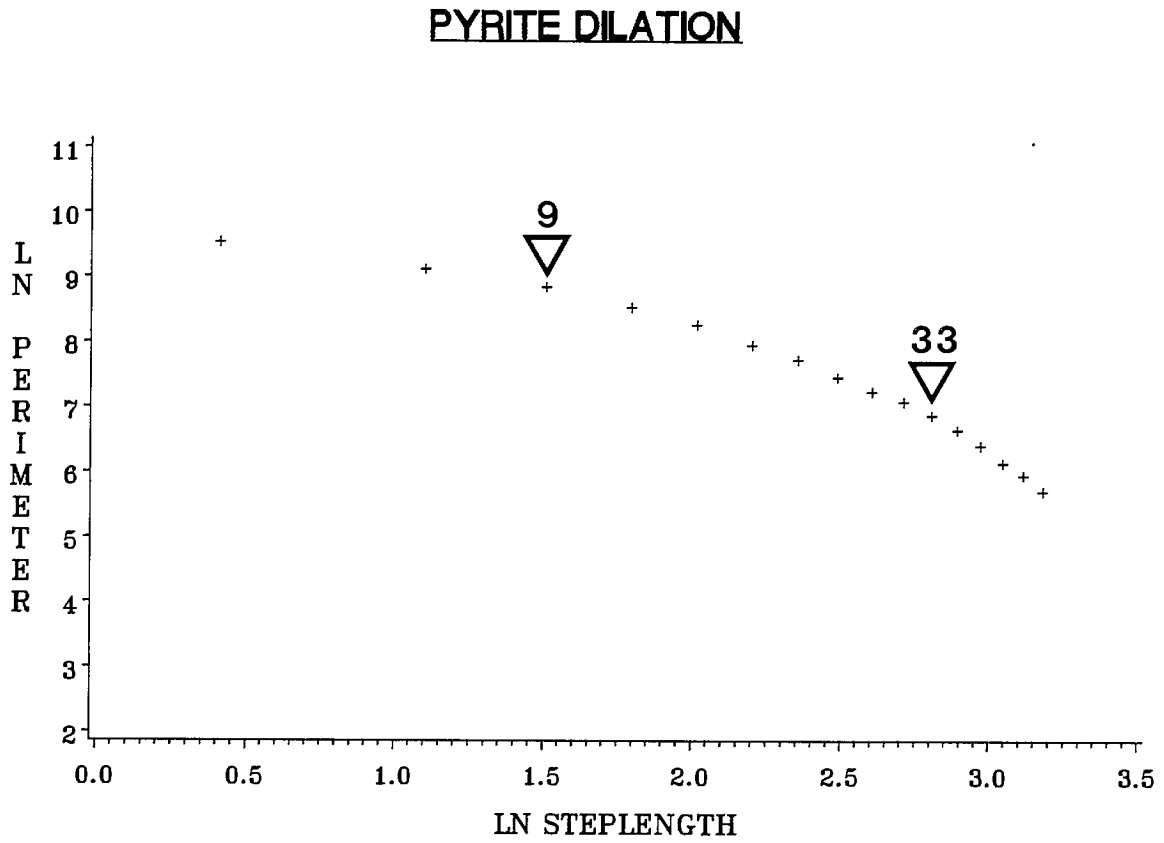

Fig. 7 – A plot of the ln perimeter versus ln steplength. Each step represents a dilation of 3 μm for each grain. The largest breaks in slope for dilation occur at 9 and 33 μm.

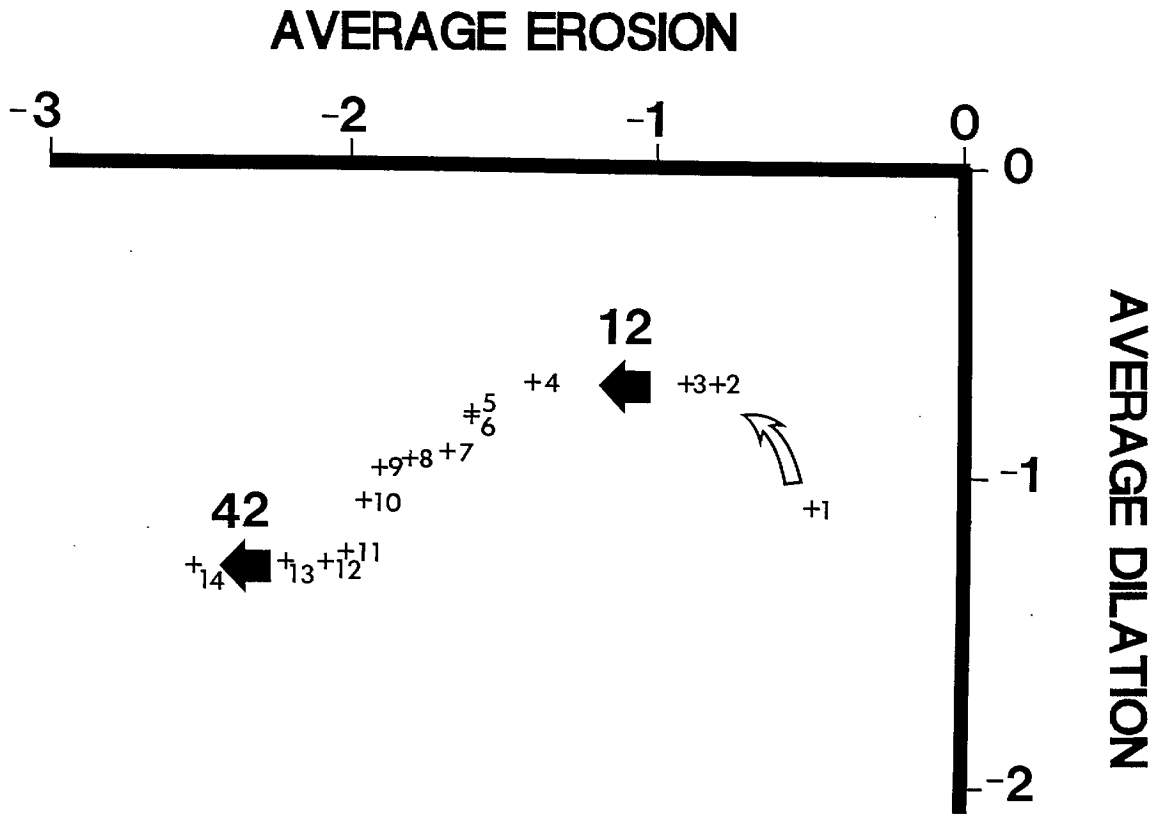

Fig. 8 – Plot of slope change for erosion versus dilation for pyrite for 210 fields (11 samples). The largest breaks in erosion occur at 12 and 42 μm. The largest break in dilation occurs at 6 μm.

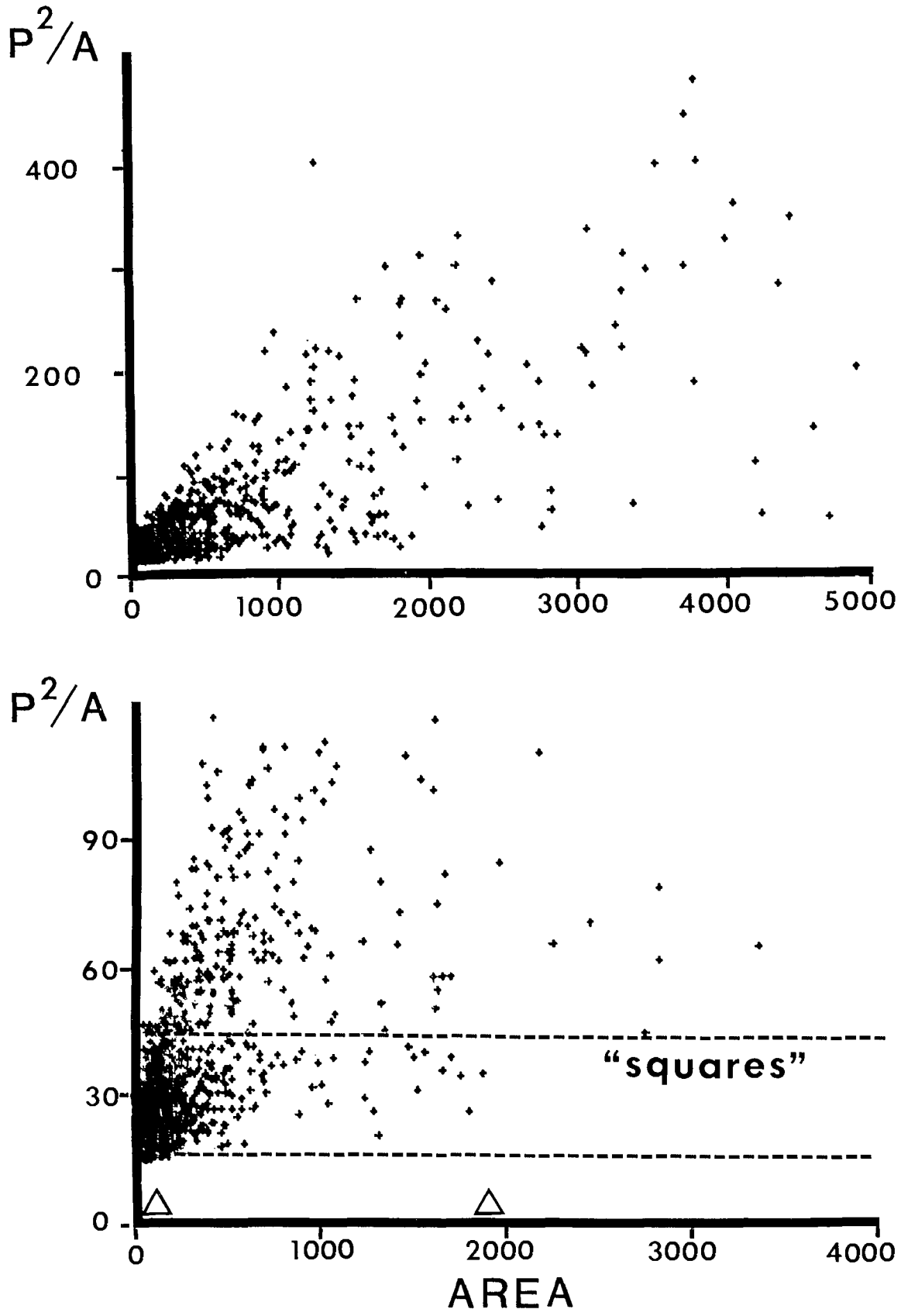

Fig. 9 – A plot of P^2/A versus Area for 1472 grains from one sample. The first plot shows the entire range for the grains analyzed. The second plot shows grains with P^2/A <100 and area <3600 (diameter = 60 μm). Horizontal lines are drawn at P^2/A = 16 and 45 to show the range for grains that appear as squares in polished sections.

some grains up to 1900 μm^2 (diameter = 44 μm) are squares; and many grains of all sizes have irregular outlines with many re–entrants (P^2/A up to 5000). The grain irregularities increase as grain size increases.

The grain diameters of 10 and 42 μm observed above correspond to the sizes noted in the grinding curves, which indicates that grain shapes and sizes also have an effect on ore breakage during grinding. The changes in the scatter diagram, however, are so subtle that the effects of grain shape on mineral breakage would not be detected if other information were not available.

DISCUSSION

Polished sections for which the erosion dilation analyses indicated changes in interrelations between grains were visually examined to determine whether the interrelations could be identified. It was observed that pyrite grains occur as individual pyrite cubes (equant grains in polished sections) and as clusters of pyrite cubes (Fig. 10). The pyrite cubes are, therefore, building blocks for the pyrite clusters. Most cubes are of two sizes, approximately 10 and 40 μm per side, although many cubes of other sizes are present. These sizes correspond to the sizes detected in the grinding tests and in the texture analyses. The interrelations of the pyrite cubes, clusters and masses confirm that the sizes, shapes, surface irregularities and separations of the pyrite grains in the BMS base metal ore influence ore breakage during grinding. The pyrite cubes are poorly, moderately and well bonded into clusters. The poorly bonded pyrite cubes form aggregates of pyrite grains in which grain outlines can be discerned by disconnected lines and points in the backscattered electron images of the pyrite in polished sections. The pyrite grains in the image can be delineated by using a grain boundary reconstruction technique with the image analyzer. The size distribution of the reconstructed pyrite grains in the image of pyrite corresponds to the size distribution of pyrite grains that were broken apart at the 15 minute grind in the laboratory ball mill.

A summary of the size and textural analyses tests (Table 3) gives three size indicators for pyrite and ground ore. The smallest size indicator ranges from 6 to 13 μm; the intermediate indicator, from 37.5 to 53 μm; and the largest one, from 106 to 150 μm. In unbroken ore the smallest size indicator corresponds to the lower size range for most pyrite crystals; the intermediate size indicator corresponds to the maximum size of most pyrite crystals; and the largest size indicator corresponds to the maximum size of pyrite clusters.

The above correlations show that the pyrite grains in a base metal ore influence ore breakage during grinding in a ball mill. In particular, the ore tends to break into particles that have the same size distribution as that of the pyrite grains in the unbroken ore. The pyrite in the unbroken ore occurs as clusters of crystals and as individual crystals. The bonding between some crystals is weak and the crystal outline is readily visible in polished sections, whereas the bonding between other crystals is strong and the crystal outline is not apparent. The poorly bonded pyrite crystals break apart during grinding of 15 minutes in a laboratory ball mill (preferential breakage). With further grinding, up to 45 minutes in a laboratory ball mill, some of the moderately bonded pyrite crystals and grains break apart (largely preferential breakage). Still further grinding breaks the particles across grain boundaries

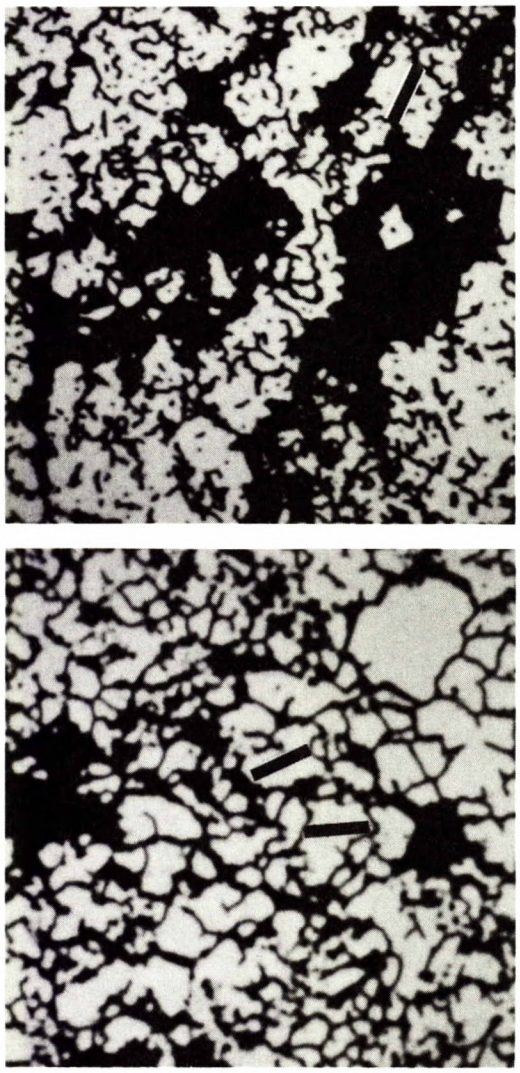

Fig. 10 – Binary images with pyrite shown in white. Scale bars on the grains represent approximately 40 μm. The width of the bar represents approximately 12 μm.

Table 3 – Summary of textural indicators

Size analyses (in μm)			
Test/Indicator	Lower	Middle	Upper
1. Ground ore	13	52	
2. Pyrite	9	37	
3. Mineral quantities		37 to 52	104 to 147
Textural analyses (in μm)			
Test/Indicator	Lower	Middle	Upper
4. Erosion			
1 scene		33, 42	
18 scenes (1 sample)		42	
210 scenes (11 samples)	6		
5. Dilation			
1 scene	9	33	
18 scenes (1 sample)	6		
210 scenes (11 samples)	6		
6. Erosion/Dilation			
average of steps (210 scenes)	6, 12	42	
7 Perimeter^2/Area vs Area			
(1472 grains, 1 sample)	<10	40	
8. Pyrite textures – cube			
sizes measured (approximate)	10	40	
Summary	6 to 13	33 to 52	

(random breakage). Size distribution curves for ground ore in a series of long grinding times (random breakage) are parallel. It is interpreted that preferential breakage occurs during the early stages of grinding, and random breakage, during the late stages. It is likely that when preferential breakage has been completed and when only random breakage occurs, there will be a good correlation between predicted and observed mineral liberations using random breakage models.

SUMMARY AND CONCLUSIONS

1. For base metal ores with high pyrite and quartz contents, such as the BMS and Trout Lake ores, screen analyses of the grinding–circuit discharge from a commercial mill and of the 15 minute grind from a laboratory ball mill correspond approximately to the size distribution of pyrite in the unbroken base metal ore.

2. Breaks in grinding curves for the BMS ore are indicated at 106 to 150, 37 to 52 and 0 to 13 μm size ranges. The breaks occur because (a) most pyrite grains are smaller than 150 μm; (b) most pyrite cubes, which are the building blocks of pyrite grains, are smaller than 42 μm; and (c) most pyrite cubes are larger than 10 μm.

3. Perimeter erosion and dilation analyses are effective rapid image–analysis techniques, which can delineate changes of interrelations among mineral grains. These changes influence ore breakage during grinding.

4. Image analysis is a reliable technique for detecting and measuring mineral properties that have a bearing on grinding in a ball mill. The technique is particularly useful because many grains must be measured to detect the appropriate mineral parameters. Once the parameters have been defined by image analysis they can be readily found by standard ore microscopy techniques.

ACKNOWLEDGEMENTS

The authors gratefully acknowledge M. Raicevic of the Mineral Processing Section, CANMET, for performing the grinding tests, and L. Surgis of BMS for supplying the ore sample. In addition, thanks are extended to the following CANMET personnel: R.G. Pinard for assistance in performing the image analysis study, M. Beaulne for preparing the polished sections, and J.D. MacLeod for drafting the figures in this report.

REFERENCES

1. Gaudin, A.M. "Principles of mineral dressing"; New York, McGraw–Hill Book Co.; 1939.

2. King, R.P. "A model for the quantitative estimation of mineral liberation by grinding"; *Int J Miner Process* 6:207–1210; 1979.

3. Klimpel, R.R. "Some practical approaches to analyzing liberation from a binary system"; *Process Mineralogy III*; edited by W. Petruk (The Society of Mining Engineers of AIME); New York, N.Y.; pp 305–311; 1986.

4. Lin, C.L., Miller, J.D., Herbst, J.A., Sepulvoda, J.E. and Prisbrey, K.A. "Prediction of volumetric abundance from two–dimensional mineral images"; *ICAM '84, Applied Mineralogy*; edited by W. Park et al. (The Society of Mining Engineers of AIME); Warrendale, Pa.; pp 157–170; 1984.

5. Finch, J.A. and Petruk, W. "Testing a solution to the King liberation model"; *Int J Miner Process* 12:305–311; 1984.

6. Petruk, W. "Predicting and measuring mineral liberations in ores and mill products, and effect of mineral textures and grinding methods on mineral liberations"; *Process Mineralogy VI*; edited by R.D. Hagni (The Society of Mining Engineers of AIME); Warrendale, Pa.; pp 393–403; 1986.

7. Petruk, W., Pinard, R.G. and Finch, J. "Relationship between observed mineral liberations in screened fractions in composite samples"; *Minerals and Metallurgical Processing* 60–62; 1986.

8. Petruk, W. "The MP–SEM–IPS image analysis system and its application to mineralogy and geochemistry"; *CANMET Report* 87–1E; 1987.

9. Petruk, W. and Schnarr, J.R. "An evaluation of the recovery of free and unliberated mineral grains, metals and trace elements in the concentrator of Brunswick Mining and Smelting Corp. Ltd."; *CIM Bulletin* 74:833:132–151; 1981.

10. Smith, M.M. and Petruk, W. "Textural classification using fractal analysis techniques"; *Proceedings of the International Symposium on the Production and Processing of Fine Particles*; CIM; Montreal (in press); 1988.

11. Flook, A.G. "The use of dilation logic on the Quantimet to achieve fractal dimension characterization of textured and structured profiles"; *Powder Technol* 21:295–298; 1987.

12. Kaye, B.H. "Specification of the ruggedness and/or texture of a fine particle profile by its fractal dimension"; *Powder Technol* 21:1; 1978.